HeLa Cell Entry by Guanidinium-Rich β-Peptides: Importance of Specific Cation–Cell Surface Interactions

ARTICLE *in* CHEMBIOCHEM · MAY 2007

Impact Factor: 3.09 · DOI: 10.1002/cbic.200600563 · Source: PubMed

4 AUTHORS, INCLUDING:

Anant K Menon
Weill Cornell Medical College
107 PUBLICATIONS **3,780** CITATIONS

DOI: 10.1002/cbic.200600563

HeLa Cell Entry by Guanidinium-Rich β-Peptides: Importance of Specific Cation–Cell Surface Interactions

Terra B. Potocky,[a, d] John Silvius,[b] Anant K. Menon,*[c] and Samuel H. Gellman*[a]

Short cationic oligomers, including arginine-rich peptides and analogous β-amino acid oligomers ("β-peptides"), can enter the cytoplasm and nucleus of a living cell from the extracellular medium. It seems increasingly clear that multiple entry pathways are possible, depending upon the structure of the guanidinium-rich molecule, the type of cell, and other factors. We have previously shown that conformational stability and spatial clustering of guanidinium groups increase the HeLa cell entry efficiency of short helical β-peptides bearing six guanidinium groups, results that suggest that these β-peptides could be useful tools for studying the entry process. Here we describe studies intended to identify the point in the entry process at which helix stability and spatial arrangement of guanidinium groups exert their effect. Our results suggest that key distinctions involve the mode of interaction between different guanidinium-rich β-peptides and the HeLa cell surface. A specific guanidinium display appears to be required for proper engagement of cell-surface heparan sulfate proteoglycans and concomitant induction of endocytic uptake.

Introduction

Short, guanidinium-rich oligomers, such as peptides with multiple Arg residues, can enter the cytoplasm and nucleus of a living cell from the extracellular medium.[1–21] This property has been exploited to generate peptide reagents that can deliver a molecular cargo to the cell interior.[22] It has been hypothesized that either entry-competent cationic peptides translocate directly across the plasma membrane into the cytoplasm[17,23–25] or that they are first endocytosed before crossing the endosomal membrane into the cytoplasm of the cell.[1–10,13–16] Although the weight of available evidence suggests that the latter pathway is more likely in many cases, specific mechanisms of entry can depend on cell type,[27] peptide sequence,[4,28] or additives,[18] and multiple pathways might operate simultaneously.

Irrespective of the mechanism of entry (direct crossing of the plasma membrane or endocytic uptake followed by crossing of the endosomal membrane), a cationic peptide must traverse a hydrophobic barrier in order to gain access to the cytoplasm of a mammalian cell. Recent evidence suggests a role for transbilayer potential in peptide translocation,[25,28,29] although there is debate on this point.[30] Silvius and co-workers showed that the cationic peptide penetratin could cross synthetic phospholipid membranes in the presence of a membrane potential,[28] while similar results were reported by Graslund and colleagues[29] in experiments designed to model the endosomal escape of penetratin. In the absence of a membrane potential, little or no peptide translocation was observed. However, Bárány-Wallje et al. were unable to detect movement of penetratin across synthetic bilayers in the presence or absence of a potential.[30] Wender et al. reported a role for membrane potential in the entry of arginine oligomers into living cells.[25]

We have exploited unique features of β-amino acid oligomers ("β-peptides") to explore the effects of molecular shape stability and of the geometry of guanidinium group display on the entry of cationic peptides into mammalian cells.[10] β-Amino acids are homologues of α-amino acids, with one additional backbone carbon atom between the amino and carboxy groups. Results from many laboratories have revealed that β-peptides can adopt a variety of regular secondary structures.[31] Of particular relevance to this work is the finding that β-peptide helices can be made much more conformationally stable than α-peptide helices, particularly at short chain lengths, and that β-peptide helix stability can be varied over a broad range by varying β-amino acid residue substitution pattern.[32,33]

The most widely studied β-peptide secondary structure is the 14-helix, which is defined by 14-membered hydrogen-

[a] *T. B. Potocky, Prof. S. H. Gellman*
Department of Chemistry, University of Wisconsin
1101 University Avenue, Madison, WI 53706 (USA)
Fax: (+1) 608-265-4534
E-mail: gellman@chem.wisc.edu

[b] *Prof. J. Silvius*
Department of Biochemistry, McGill University
Montreal, Quebec H3G 1Y6 (Canada)

[c] *Prof. A. K. Menon*
Department of Biochemistry, Weill Medical College of Cornell University
1300 York Avenue, New York, NY 10021 (USA)

[d] *T. B. Potocky*
Current address: Department of Biology, Boston College
140 Commonwealth Avenue, Chestnut Hill, MA 02467

bonded rings between backbone groups [C=O(*i*)–H–N-(*i*−2).[31,34–36] β-Peptides made up of β^3-residues (i.e., residues that bear a side chain on the backbone carbon adjacent to the nitrogen atom) often display 14-helical conformations in organic solvents but seldom fold in aqueous solution. The cyclically constrained β-amino acid *trans*-2-aminocyclohexanecarboxylic acid (ACHC), on the other hand, has a very high propensity for the 14-helical conformation, even in water.[32,33,38] The combination of rigid ACHC residues and flexible β^3-residues bearing specific side chains generates β-peptides that form stable helices and display particular three-dimensional arrangements of functional groups.[10] This feature enables easy exploration of relationships among function, molecular shape, and geometry of side-chain display in sets of short β-peptides. Analogous studies are difficult or impossible to conduct among short arginine-rich α-peptides because secondary structure is much more difficult to control in these molecules.

Previous work from our laboratory and others has established that β-peptides composed largely or entirely of β^3-homoarginine (β^3-hArg) residues display a profile of cell-entry activity very similar to that of Arg-rich α-peptides.[2,10,19–21] Both types of cationic oligomer, for example, move into live cells through an ATP-dependent process that provides access to the cytoplasm and the nucleus.[2] In both cases, hindrance of endosome acidification blocks movement from endosomes into the cytoplasm.[2] The results presented below, in concert with recent reports on cationic α-peptides, strengthen the analogy between β-peptides rich in β^3-hArg and α-peptides rich in Arg. Mechanistic conclusions drawn from studies with β-peptides could therefore apply to analogous α-peptides.

We have previously compared the secondary structures and cell entry efficiencies of β-peptides **1**, **2**, and **3** (which was designated **5** in our previous report;[10] the lower case letter following the numerical peptide designation indicates a particular N-terminal reporter group: a = β^3hTyr, b = fluorescein, *c* = 7-nitrobenz-2-oxa-1,3-diazol-4-yl (NBD)). Sequence isomers **1a** and **3a** adopt the 14-helical conformation in aqueous solution; the guanidinium side chains of **1a** are thus clustered along one side of the helix, while the guanidinium side chains of **3a** are dispersed around the entire helix periphery. β-peptide **2a**, which is comprised entirely of flexible β^3-residues, does not adopt a 14-helical conformation in aqueous solution, but folding occurs in methanol or in the presence of dodecylphosphocholine (DPC) micelles. The helical conformations of **1** and **2** are analogous in that both feature guanidinium side-chain clustering. When we evaluated the abilities of **1b**, **2b**, and **3b** to enter live HeLa cells, we found that only **1b** entered efficiently. Cells exposed to **2b** or **3b** displayed weak, mostly punctate fluorescent staining, which we interpreted as indicating low levels of endocytic uptake. Entry of **1b** could be arrested at the vesicle stage (no movement into the cytoplasm or nucleus) by treatment of cells with NH_4Cl,[10] as we had previously observed for a Tat-derived α-peptide and a related β-peptide.[2] Chmielewski et al. have designed proline-rich peptides to address similar questions regarding geometry of guanidinium display (ref. [39]; for previous work on proline-derived systems by Giralt et al., see refs. [40,51] and references therein).

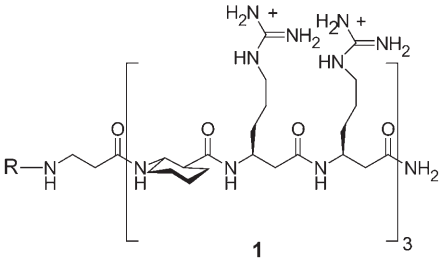

1

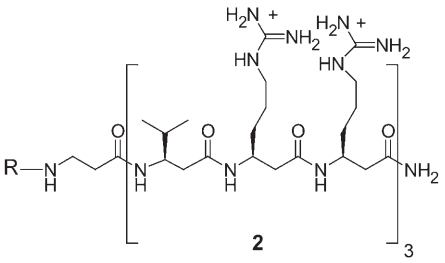

2

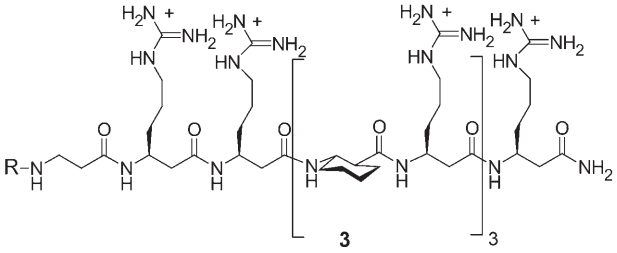

3

Series **a**: R = β^3hTyr
Series **b**: R = Fluorescein
Series **c**: R = NBD

Here we describe experiments that were designed to provide insight on the pathway by which carboxyfluorescein-labeled β-peptides enter HeLa cells. On the structural level, differences among **1**–**3** are subtle; nevertheless, these compounds display substantial differences in behavior, which makes them very useful for mechanistic analysis. Our goal is to identify the point(s) in the entry pathway at which the differences in conformational stability and geometry of guanidinium display among **1**–**3** are manifested.

Results and Discussion

β-Peptide entry pathway

Our previous results had suggested that entry-competent β-peptides enter HeLa cells by some form of endocytosis and then escape from the endosomal compartment to enter the cytoplasm and nucleus.[2,10] To analyze the entry pathway further we used experimental approaches that have been employed by other groups in the study of arginine-rich α-peptides.[4,5,8,9,14] First, we expressed a dominant negative mutant

of dynamin-1 (Dyn1 K44A)[5,41,42] in HeLa cells and then determined whether a β-peptide could enter cells that were unable to endocytose Texas Red-labeled transferrin (TR-Tf). The inability to endocytose TR-Tf is diagnostic for cells in which the clathrin-mediated endocytic pathway has been disrupted by expression of Dyn1 K44A. This experiment has a built-in control, since only ~30% of the cells are transformed; transformed cells are identified by the inhibition of TR-Tf internalization, and these cells can be independently assessed for entry of carboxyfluorescein-labeled β-peptide because of the difference between the wavelengths of maximum fluorescence emission intensity of carboxyfluorescein and Texas Red.

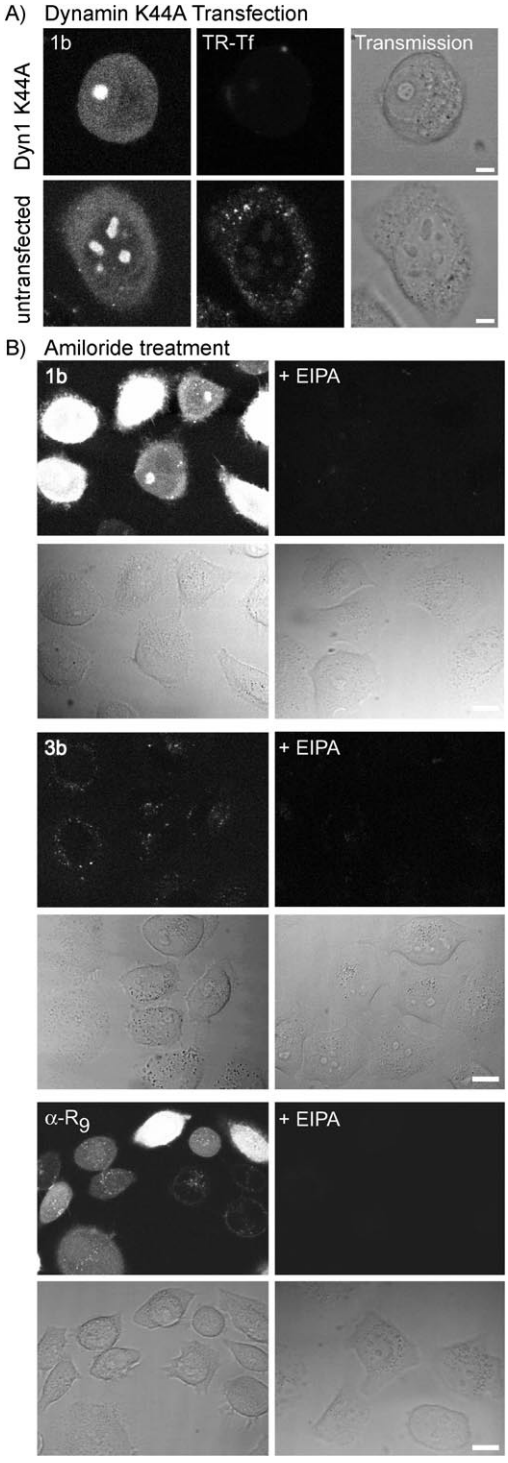

Figure 1 A shows representative confocal fluorescence micrographs from this experiment. Confocal microscopy was crucial as an analytical tool because it allowed us to distinguish internalized fluorescence in endosomes from internalized fluorescence dispersed in the cytoplasm or localized in the nucleus. Among the cells in which TR-Tf endocytosis was inhibited because of Dyn1 K44A expression, approximately 50% retained the ability to take up β-peptide **1b**. This level of uptake is only slightly less than the ~70% uptake level observed for cells in which TR-Tf uptake is unimpaired (i.e., cells with little or no expression of Dyn1 K44A cDNA; Figure 1 A, bottom panels). Similar results were obtained with the K44A mutant form of dynamin-2,[42] the dynamin isoform found in most mammalian cells. In a direct α-peptide comparison, we observed unimpeded entry of carboxyfluorescein-labeled α-arginine 9-mer in cells expressing Dyn1 K44A or Dyn2 K44A (data not shown), which is consistent with findings of Wadia et al. for a Tat-tagged protein.[5] These results indicate that β-peptide **1b** is endocytosed predominantly by a dynamin-independent pathway, although a small fraction of the material appears to be taken up through dynamin-dependent (clathrin-mediated) endocytosis.

In a second set of experiments designed to probe the mechanism of β-peptide uptake, we used ethyl isopropyl amiloride (EIPA), an agent that has been used to block macropinocytosis.[43–44] EIPA has been reported to inhibit EGF-stimulated macropinocytosis while having no effect on clathrin-mediated endocytosis of EGF itself[48] and has been used to examine uptake of arginine oligomers into HeLa cells,[4] although caution in the interpretation of results from such experiments has recently been advocated.[14] We found that HeLa cells treated with EIPA were able to internalize TR-Tf (data not shown), a process that is believed to involve clathrin-mediated endocytosis; this result is consistent with precedents that indicate that EIPA does not inhibit clathrin-mediate endocytosis.[48] HeLa cells pretreated with EIPA (100 μM) for 30 min were incubated with β-peptide **1b** or **3b** for 60 min at 37 °C. Unlike untreated cells, EIPA-treated cells showed virtually no uptake of **1b** into the cytoplasm, nucleus, or endocytic vesicles (Figure 1 B; this dark image establishes that fluorescence observed for cells treated in other

Figure 1. A) Evaluation of the role of dynamin in the uptake of β-peptide **1b**. HeLa cells were transfected with Dyn1 K44A by use of TransIT® transfection agent (Mirus). The cells were allowed to recover for 24 h after transfection and were then incubated with **1b** (8 μM) and TR-Tf (5 μg mL^{-1}) for 30 min at 37 °C. The cells were washed and then viewed by confocal microscopy. The ability of cells to internalize TR-Tf was used to determine whether they had been transfected with Dyn1 K44A, as indicated by inhibition of TR-Tf uptake. Cells transfected with Dyn1 K44A efficiently internalized **1b**. A cell transfected with Dyn1 K44A (top) and an untransfected cell (bottom) show similar levels of uptake of **1b**. Bar: 10 μm. B) Effect of amiloride treatment on the uptake of **1b** and **3b**. HeLa cells were pretreated with EIPA (100 μM) for 30 min at 37 °C. The medium was replaced with β-peptide (8 μM) in the presence of EIPA (100 μM) and the cells were incubated for 1 h at 37 °C, washed, and then viewed by confocal microscopy. Cells were incubated with **1b** (top four panels) or **3b** (bottom four panels) in the absence (left) or presence (right) of EIPA. Uptake of β-peptides **1b**, **2b** (not shown), and **3b** was inhibited in amiloride-treated cells. Each experiment was repeated three or more times with similar results. Bar: 10 μm.

ways—with **1b** in the absence of EIPA, for example—reflects β-peptide entry rather than background or autofluorescence). Approximately 60% of the cells displayed β-peptide uptake in the absence of EIPA, but this proportion decreased to ~5% in the presence of EIPA. Similar levels of inhibition were observed for Flu-α-R_9 in EIPA-treated cells, decreasing from ~70% in the absence of EIPA to ~10% in the presence of EIPA (Figure 1B). Other groups have reported that EIPA inhibits cellular uptake of arginine-rich α-peptides,[4,5,9] although the mechanistic significance of such observations has recently been questioned.[14] Consistent with our previous report,[10] β-peptides **2b** (not shown) and **3b** displayed only weak staining of endocytic vesicles, and no staining of the cytoplasmic or nuclear compartments, in untreated cells the endocytic staining observed with **3b** is most easily seen in the inset enlargement. We interpret this behavior as indicating that the entry of these β-peptides is so inefficient that only in endocytic vesicles is the concentration high enough to allow detection. The weak punctate staining displayed by **2b** and **3b** was blocked in EIPA-treated cells, indicating that EIPA inhibited not only cytoplasmic and nuclear translocation of β-peptides as seen with **1b**, but also β-peptide accumulation in endocytic vesicles, which we regard as the first step in the entry process.

The results shown in Figure 1 indicate that a dynamin-independent, amiloride-sensitive endocytic pathway is a major route by which β-peptide **1b** enters HeLa cells. Similar conclusions have been reached for arginine-rich α-peptides in several cases[4,5,9] (see also our results with Flu-α-R_9), although not universally.[14,17] Our observations are consistent with macropinocytosis as a major pathway for cell entry; however, the data allow for a significant clathrin-mediated entry pathway as well. After uptake of β-peptide **1b** in macropinosomes and/or other vesicles the β-peptide must subsequently escape from these vesicles in order to gain access to the cytoplasm and nucleus of the HeLa cell (discussed below).

β-Peptide 1b induces actin reorganization

Macropinocytosis is not a constitutive process in most mammalian cells and occurs only upon stimulation by growth factors, mitogens, or small molecules such as phorbol esters.[43] We therefore considered the possibility that β-peptide **1b** is able to stimulate macropinocytosis and thus induce its own uptake. In an important precedent, Nakase et al. found that oligomers of α-arginine induce actin reorganization in HeLa cells;[4] actin reorganization is frequently interpreted as an indication of macropinocytic stimulation.[43] We examined the effects of β-peptide treatment on the distribution of actin in HeLa cells by fixing and permeabilizing treated cells and staining with Alexafluor 488 phalloidin, following previous work.[4] Serum-starved HeLa cells were incubated with 8 μM nonfluorescently labeled β-peptide (**1a**, **2a**, or **3a**) or 10 nM EGF (a positive control known to induce actin reorganization) for 30 min, fixed, stained with AlexaFluor 488 phalloidin, and visualized by confocal fluorescence microscopy. Serum-starved cells that had not been treated with β-peptide or EGF were analyzed in parallel (negative control). A cell in a resting, nonmitotic state will generally display a filamentous distribution of actin fibers across the length of the cell (Figure 2A), whereas a stimulated cell or a cell undergoing mitosis will no longer display actin filaments across the entire cell, but will instead display actin filaments localized to the edges of the cell (Figure 2B).[43,49] The number of cells displaying normal and reorganized actin filaments after treatment with β-peptide or EGF was assessed by cell counting (Figure 2C).

Approximately 20% of untreated HeLa cells showed reorganized actin filaments (as illustrated in Figure 2B); these cells were most probably undergoing cell division, a process that requires actin reorganization. The proportion of cells with reorganized actin filaments increased to approximately 50% upon treatment with EGF. Actin reorganization was observed also upon treatment of cells with β-peptide **1a** (Figure 2B), while

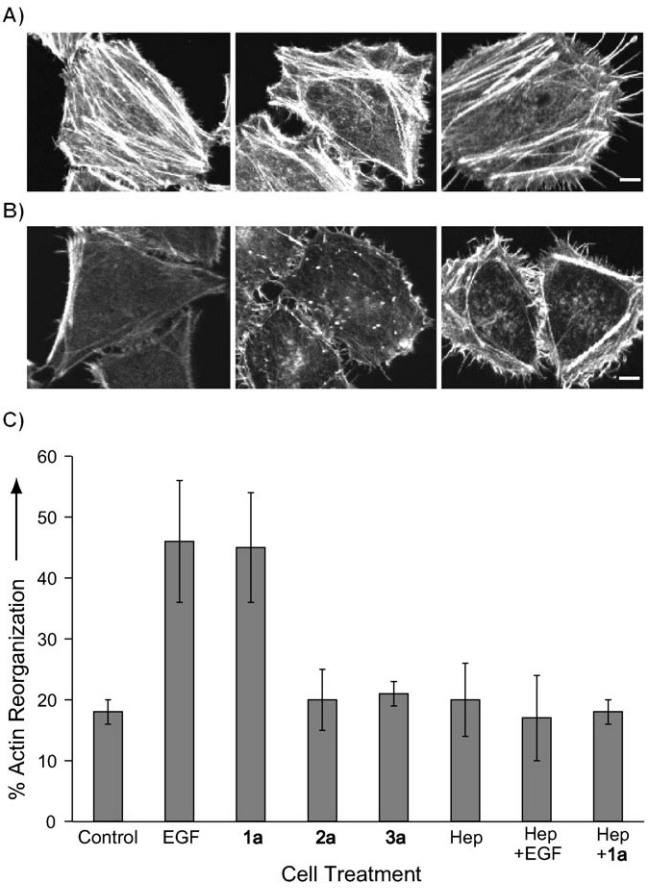

Figure 2. Actin reorganization of cells treated with **1a**, **2a**, **3a**, or EGF. Serum-starved cells were incubated either with serum-free medium alone or with serum-free medium containing non-carboxyfluoresceinated β-peptide or EGF for 30 min at 37 °C. The cells were then washed, fixed, permeabilized, and stained with Alexa Fluor 488 phalloidin. The cells were viewed by confocal microscopy. A) Examples of HeLa cells showing normal filamentous actin staining; cells in all three panels were serum-starved and then stained with phalloidin. Bar: 10 μm. B) Examples of HeLa cells with reorganized actin filaments; cells in the left two panels were treated with EGF (10 nM); cells in the right panel were treated with β-peptide **1a** (8 μM). Bar: 10 μm. C) Quantification of cells showing actin reorganization upon treatment with β-peptide or EGF. Actin reorganization in heparinase III-treated (Hep-treated) cells is also shown. Both EGF and **1a** induce actin reorganization in HeLa cells. Induction of actin reorganization by EGF or **1a** is inhibited in heparinase III-treated cells.

treatment with β-peptide **1b** gave similar results, indicating that attachment of the fluorophore to the β-peptide (as in **1b**) does not affect its ability to induce actin reorganization (data not shown). β-Peptides **2** and **3**, which are unable to enter HeLa cells efficiently, were tested for their ability to induce actin reorganization. Cells treated with either **2a** or **3a** displayed actin distributions comparable to that of the negative control (Figure 2C). These results suggest that the conformational rigidity and amphiphilicity of β-peptide **1** are required for induction of actin reorganization, and that the ability to induce actin reorganization is correlated with efficient HeLa cell entry.

It is widely accepted that cationic oligomers interact electrostatically with heparan sulfate proteoglycans (HSPs) on the cell surface.[4,7,8,50–55] We explored the role of this interaction in the induction of actin reorganization. Cells were treated with heparinase III,[46] washed extensively, and then treated with β-peptide **1a**. Under these conditions the percentage of cells treated with β-peptide **1a** that displayed reorganized actin dropped to that of control cells treated solely with heparinase III; a comparable diminution of actin reorganization was seen for cells treated with heparinase III followed by EGF (Figure 2C). Of the three β-peptide sequences evaluated in this study, only the one that adopts a stable 14-helical conformation and displays a focused guanidinium cluster (i.e., **1**) allowed the interaction with HSPs that is necessary for actin reorganization. This specificity is striking in view of our earlier finding that all three of these guanidinium-rich β-peptides bind to the HeLa cell surface.[10] Together, our previous and current results suggest that propagation of the signal that triggers actin reorganization, a signal that must pass from the cell surface to the cytoplasm, requires a specific interaction between an oligocation and HSPs. Our data suggest that **1** is superior to the other two β-peptide sequences in forming this specific, actin reorganization-triggering interaction.

Translocation of β-peptides 1, 2, and 3 across the bilayers of synthetic liposomes

The conclusions outlined above regarding entry into HeLa cells require that the β-peptides ultimately traverse the endosomal membrane to gain access to the cytoplasm. We evaluated the ability of β-peptides to traverse phospholipid bilayers as a model system for crossing a biological membrane. β-Peptides **1c**, **2c**, and **3c**, each bearing an N-terminal 7-nitrobenz-2-oxa-1,3-diazole (NBD) fluorophore, were used in these studies. Vesicles of four different phospholipid compositions—POPC/POPG (1:1 mol/mol), POPC/POPG (3:1), POPC/POPS (3:1), or POPC/soy PI (3:1)—were prepared and treated with the potassium ionophore valinomycin to produce a transbilayer membrane potential. The ability of β-peptides to enter the vesicles was determined by destroying the extracellular fluorescence with dithionite, a membrane-impermeant molecule that reduces the nitro functionality on NBD to an amine, rendering the molecule nonfluorescent. By comparing the fluorescence of vesicle/β-peptide samples before and after dithionite treatment, we were able to assess the fraction of β-peptide inaccessible to dithionite reduction (i.e., the fraction that had translocated into the vesicles).[26,28] As we have shown previously for α-Arg oligomers,[28] these lipid compositions allow peptide translocation to be measured under conditions in which the cationic peptide molecules are almost entirely bilayer-bound (vide infra), which is essential to determine accurate rate constants for the potential-dependent translocation of these peptides across bilayers (compare, e.g., refs. [28] and [30]). Furthermore, decay of the transbilayer potential is relatively slow over the time course examined for these lipid compositions. These features allow accurate comparisons of the initial rates of potential-dependent translocation among the different β-peptides, without the complicating effects of unequal extents of binding of different β-peptides to the vesicles or rapid decay of the transbilayer potential. Moreover, the 3:1 PC/PS, PC/PG, and PC/PI vesicles carry surface charges comparable to those manifested by eukaryotic cell membranes. However, as we have shown previously, bilayers with a wide variety of other lipid compositions support potential-dependent translocation of polycationic peptides comparable to those examined here.[28]

In the absence of a transbilayer potential, the majority (>94%) of β-peptide incubated with either POPC/POPS or POPC/POPG (3:1 mol/mol) vesicles remained in the dithionite-accessible extravesicular space, even after a 36 h incubation period (not shown). In the presence of a transbilayer potential, however, all three β-peptides (**1c–3c**) entered the vesicles and were protected from dithionite (Figure 3A). The initial rate of β-peptide internalization, as well as the rate of internalization of a representative α-peptide, α-R_6GC–NH_2, was determined in each vesicle system (Table 1). All three β-peptides entered POPC/POPS (3:1) vesicles with similar efficiencies, while β-peptides **1c** and **3c** entered POPC/POPG (3:1) and POPC/POPG (1:1) vesicles more efficiently than did **2c**. β-Peptide **3c** entered POPC/soy PI (3:1) vesicles with an initial rate roughly twice that of **1c** or **2c**. Overall, the data indicate that there is no simple correlation between the ability of a β-peptide to move across a lipid bilayer and either the conformational stability of the β-peptide helix or the way in which guanidinium side chains are spatially arranged.

Effective dissociation constants were determined for binding of the three β-peptides and of α-R_6GC–NH_2 to each type of lipid vesicle mentioned above (Figure 3B, Table 1). There does not appear to be any correlation between the ability of a β-peptide to bind to the surface of a vesicle and the ability of that β-peptide to translocate across the vesicle membrane. For example, **3c** bound to POPC/POPS and POPC/soy PI vesicle surfaces with much lower affinity than **2c**, but **3c** was internalized into these vesicles at a considerably higher initial rate than was **2c**. The data thus suggest that the rates at which cationic β-peptides translocate across synthetic vesicles do not depend upon the affinities with which they bind to anionic lipid surfaces.

EGF stimulation of the uptake of β-peptides 2 and 3

The synthetic vesicle studies show that β-peptides **2c** and **3c** can cross a membrane bilayer that has a potential imposed

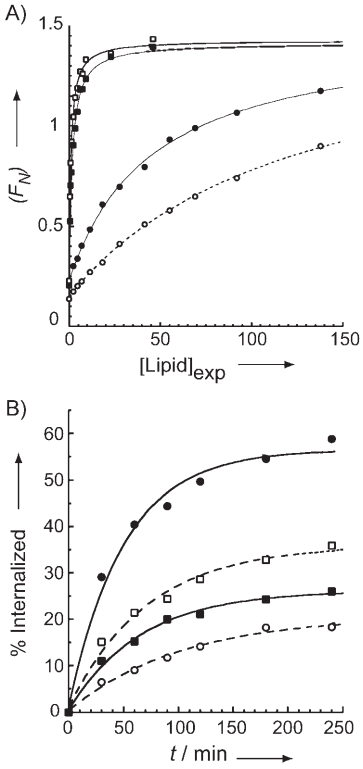

Figure 3. Translocation of β-peptides across liposomal membranes. A) Binding of NBD-labeled α or β-peptides to POPC/soy PI (3:1 mol/mol) large unilamellar vesicles. Peptides (0.1 nmol) and lipid vesicles at varying concentrations were incubated at 37 °C in Na^+ buffer (3 mL) for 30 min, the fluorescence was then determined before and after addition of excess sonicated POPG vesicles, and the normalized fluorescence (F_N) was calculated as described in the Experimental Section. The resulting data are plotted as a function of the concentration of surface-exposed LUV lipid added ($[lipid]_{exp}$, determined as described in the Experimental Section), and are fitted to an equation of the form $F_N = F_N^0 + (F_N^{max} - F_N^0)\,([lipid]_{exp}/(K_d + [lipid]_{exp}))$, where F_N^0 and F_N^{max} are the values of F_N for free and lipid-bound peptide, respectively. Data shown are from a single representative experiment, which yielded these values for the dissociation constant K_d: 125 ± 8 μM for α-R_6GC-NH_2 (○), 1.00 ± 0.07 μM for **1c** (□), 1.63 ± 0.15 μM for **2c** (■), and 46 ± 3 μM for **3c** (●). Data from replicate experiments are summarized in Table 1. B) Potential-driven translocation of NBD-labeled peptides into POPC/soy PI LUV (3:1 mol/mol) at 37 °C. LUVs and peptide (3 mM and 3 μM, respectively) were co-incubated at 37 °C, and the percentage of total peptide (% internalized) into the vesicles after various times was determined by the dithionite-reduction method described in the Experimental Section. Data shown are from a single representative experiment, which gave the following initial rates of peptide internalization: 11.9 ± 2.1 % h^{-1} for α-R_6GC–NH_2 (○), 29.3 ± 4.5 % h^{-1} for **1c** (□), 23.5 ± 2.5 % h^{-1} for **2c** (■), and 66.0 ± 9.4 % h^{-1} for **3c** (●). Data from replicate experiments are summarized in Table 1.

Table 1. Lipid binding constants and rates of potential-driven translocation for α and β-peptides.[a]

Peptide	Lipid mixture PC/PS 3:1	PC/PG 3:1	PC/PI 3:1	PC/PG 1:1
	K_d [μM]			
R_6GC(NBD)-NH_2	44 ± 6	71 ± 7	113 ± 15	< 10[b]
1c	1.0 ± 0.4	1.0 ± 0.1	1.2 ± 0.2	< 5[b]
2c	1.5 ± 0.3	1.7 ± 0.3	2.1 ± 0.4	< 5[b]
3c	31 ± 3	30 ± 4	42 ± 4	< 5[b]
	Initial rate of potential-driven uptake [% h^{-1}]			
R_6GC(NBD)–NH_2	2.5 ± 0.9	2.0 ± 0.3	8.6 ± 1.4	2.0 ± 0.4
1c	9.0 ± 2.8	20.6 ± 2.1	52.0 ± 13.2	25.6 ± 1.1
2c	6.5 ± 2.3	13.6 ± 2.0	34.8 ± 6.4	11.7 ± 1.7
3c	10.5 ± 13.2	27.1 ± 4.7	88.6 ± 16.0	32.9 ± 1.6

[a] Values listed represent (except where otherwise indicated) the means ± SEMs of three independent experiments carried out and analyzed as described in Experimental Section. [b] Values of K_d were estimated in a single experiment as 7.0 ± 0.5 μM, 3.7 ± 0.4 μM, < 1 μM, and 4.7 ± 0.3 μM for R_6GC–NH_2, **1c**, **2c**, and **3c**, respectively.

across it; however, the HeLa cell studies show that neither **2** nor **3** induces actin reorganization or undergoes efficient cell entry. We therefore considered the possibility that stimulation of macropinocytosis by an independent reagent might increase the extent to which β-peptides **2** and **3** would enter Hela cells. Stimulation of macropinocytosis by EGF, for example, would perhaps allow entry of β-peptides **2** and **3** into macropinosomes, since previous work has shown that these β-peptides can bind to the HeLa cell surface.[10] Once internalized into these vesicles, β-peptides **2** and **3** should be able to translocate across the vesicular membrane to enter the cytoplasm, according to the vesicle model study results. We tested this hypothesis by exposing HeLa cells to **2b** or **3b** together with EGF (10 nM). This conincubation resulted in significant cytoplasmic accumulation of each β-peptide (Figure 4), but both

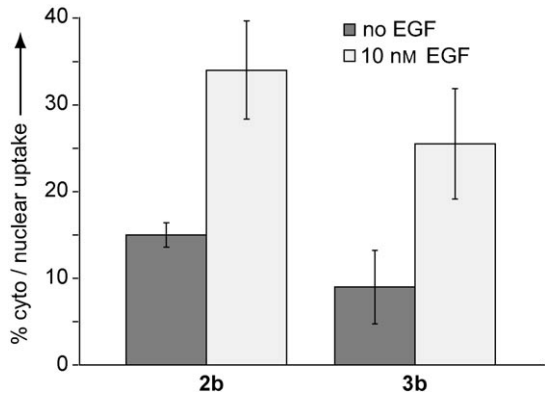

Figure 4. EGF stimulation of β-peptide uptake. Cells were treated with **2b** or **3b** (8 μM) either in the absence (dark gray bars) or in the presence (light gray bars) of EGF (10 nM) for 1 h at 37 °C. The cells were then washed and viewed by confocal microscopy. The number of cells with nuclear and cytoplasmic staining (% cyto/nuclear uptake) was counted. The data are each the average of two independent experiments. Error bars denote standard deviation.

2b and **3b** displayed lower accumulation in the cytoplasm of EGF-treated cells than had β-peptide **1b** in the absence of EGF treatment; this suggests that β-peptide **1b** might be more efficient than EGF in stimulating macropinocytosis. Our coincubation results indicate that **2b** and **3b** can cross an intracellular vesicle membrane subsequent to EGF-stimulated uptake; this is consistent with the ability of these β-peptides to move spontaneously across liposome bilayers in the presence of a transmembrane potential.

Conclusions

Our data suggest that β-peptide **1** induces HSP-dependent actin reorganization in HeLa cells and that this molecule enters the cells at least in part by a dynamin-independent, amiloride-sensitive, endocytic pathway that displays the characteristics of macropinocytosis. Other endocytic entry pathways might operate as well. In contrast, β-peptides **2** and **3** do not induce actin reorganization, and do not enter cells as efficiently as does **1**. It is intriguing that the functional distinction, **1** versus **2** and **3**, is not maintained in synthetic liposomes: all three β-peptides spontaneously enter synthetic vesicles of several different phospholipid compositions in the presence of a membrane potential. Stimulation of macropinocytosis by EGF results in cell entry by **2** or **3**; this suggests that once they have been internalized into macropinosomes, these two β-peptides are able to cross the macropinosomal membrane.

Our present and previous observations[2,10] suggest that β-peptides gain access to the cytoplasm and nucleus of a HeLa cell mainly by way of some type of endosomal compartment rather than by direct crossing of the plasma membrane. Since we show here that all three β-peptides can move spontaneously across synthetic lipid bilayers in the presence of a transbilayer potential, one might wonder why the β-peptides do not move spontaneously across the plasma membrane of a HeLa cell. One possible explanation is that the rate of β-peptide endocytosis is higher than the rate of translocation across the outer membrane. Another possibility is that movement across the outer cell membrane, as opposed to a synthetic lipid bilayer, requires dissociation from membrane proteoglycans,[29,50] which must be assisted either by the reduced pH of the endosome or by degradation of the carbohydrates in the endosome.[50] A third possibility is that differences in lipid composition between the macropinosomal and/or other endosomal membranes on one hand and plasma membranes on the other lead to more rapid translocation across the former than the latter. The activity differences among **1**, **2**, and **3** that we observe with live HeLa cells and the contrasting activity similarities with synthetic vesicles indicate that the ability of an oligocation to cross a synthetic bilayer is not sufficient to explain entry of that oligocation into living cells. It should be noted that Shen et al. have used a novel cell fractionation strategy to examine the mechanism by which cationic α-peptides enter cells,[17,24] and these workers have concluded that the major entry pathways do not require endocytic processes but rather involve direct crossing of the plasma membrane. These conclusions do not agree with those drawn by a number of other groups (including us),[1–16] and the origin of these differences is not clear at present. Since our data show that β-peptides **2** and **3** can move across lipid bilayers but do not enter live HeLa cells efficiently, these molecules might be interesting subjects to examine by the cell fractionation method.

The results reported here suggest a specific role for heparan sulfate proteoglycans in the entry mechanism of guanidinium-rich β-peptides. The apparent requirement for HSP involvement in uptake has been attributed by many to an electrostatic attraction between the negatively charged proteoglycan and the positively charged peptide that simply draws the oligocation to the cell surface.[4,7,8,51,53–55] Our data, however, suggest that oligocation binding to the HeLa cell surface alone is insufficient to induce uptake. Instead, the negatively charged proteoglycan appears to play a more complex role: this material might serve as a cell-surface receptor that, when engaged by a molecule displaying an appropriate spatial arrangement of guanidinium groups, mediates the induction of actin reorganization and ultimately macropinocytosis (and/or other forms of endocytosis). This hypothesis is consistent with evidence that the activity of signaling proteins can be modulated by variations in HSP structure;[52] to our knowledge our results are the first to suggest that cell entry by unnatural oligocations depends upon the structural features of their interactions with HSP. It seems likely that the conclusions we have drawn for β-peptides are relevant also for arginine-rich α-peptides, since previous work (e.g., ref. [2]) and results discussed above demonstrate considerable similarity between the entry processes at work in each case. The uptake mechanism might vary from one cell type to another. Here we have studied only HeLa cells, but our results suggest that β-peptides **1**–**3** represent useful tools for analysis of entry pathways active in other cell types. (While this paper was under review, Nakase et al. published a report suggesting that interaction between arginine-rich α-peptides and HSP is necessary to induce actin reorganization and macropinocytosis in CHO cells.[56])

Experimental Section

α and β-peptide synthesis and labeling: All β-peptides were synthesized in parallel by manual Fmoc solid-phase synthesis on Novasyn TGR resin. Couplings were performed over a course of 3 h by using *O*-benzotriazol-1-yl-*N*,*N*,*N*′,*N*′-tetramethyluronium hexafluorophosphate (HBTU) (3 equiv), hydroxybenzotriazole (HOBt; 3 equiv), and DIEA (6 equiv) in DMF. Deprotections were performed in piperidine/DMF (20%). Double couplings were employed for the second and third (*S*,*S*)-ACHC residues in **1**. A β-homoglycine (βhGly) linker was conjugated to the N terminus of each β-peptide on resin. The β-peptide on half of the resin was then coupled to 6-carboxyfluorescein [HBTU/HOBt (3 equiv), DIEA (9 equiv)] for 12 h. The remaining resin was coupled to Fmoc-β^3hTyr, which was followed by Fmoc deprotection. β-Peptides were cleaved from resin by use of TFA (92.5%) with thioanisole (5%) and ethanedithiol (2.5%) for 5 h. All β-peptides were purified by preparative reversed-phase high-pressure liquid chromatography (RP-HPLC) on a Vydac C4 silica column with use of a nonlinear gradient of water/acetonitrile containing TFA (0.1% *v*/*v*). β-Peptide identity was evaluated by matrix-assisted laser desorption ionization time-of-flight (MALDI-TOF) analysis on a Bruker Reflex II instrument. Expected molecular weights $[M+H]^+$ are as follows: β-peptide **1a** (1662.1), β-peptide **1b** (1842.1), β-peptide **1c** (1648.0), β-peptide **2a** (1626.1), β-peptide **2b** (1807.1), β-peptide **2c** (1612.0), β-peptide **3a** (1662.1), β-peptide **3b** (1842.1), and β-peptide **3c** (1648.0). The purified β-peptides were lyophilized and redissolved in water. Concentrations were determined by UV/visible spectroscopy at 494 nm (fluoresceinated β-peptides: $\varepsilon = 68000$ at pH 7.4) or 275 nm (β^3-homotyrosine-containing oligomers: $\varepsilon = 1420$).

The α-peptide Flu-α-R_9 was synthesized and purified in an analogous manner to the β-peptides described above. The α-peptide

$R_6GC–NH_2$ was synthesized and labeled on its C-terminal cysteine residue with *N,N'*-dimethyl-*N*-(iodoacetyl)-*N'*-(7-nitrobenz-2-oxa-1,3-diazol-4-yl)ethylenediamine (IANBD)-amide as described previously.[28]

Cell cultures: HeLa cells were cultured in Dulbecco's modified Eagle Medium (DMEM) supplemented with fetal bovine serum (FBS; 10% *v/v*), penicillin (100 units mL^{-1}), and streptomycin (100 μg mL^{-1}) in a humidified incubator under 5% CO_2 gas.

Confocal microscopy: HeLa cells grown to subconfluence on 90 mm plates were dissociated over a course of 15 min at 37 °C by treatment with trypsin/EDTA. Cells (10^5 per well) were plated onto 35 mm glass-bottomed culture dishes (MatTek) and cultured overnight in DMEM with FBS (10%) and pen/strep. The cells were then treated for the various experiments as described below. The cells were viewed by confocal microscopy by use of a BioRad MRC 1024 laser scanning confocal microscope with excitation/emission wavelengths set at 488/522 nm for fluorescein and 568/605 nm for propidium iodide. Peptide uptake was quantitated by cell counting. We distinguished among cells displaying only endosomal uptake (punctate fluorescence pattern), cells displaying cytoplasmic staining (diffuse fluorescence), and cells displaying nuclear localization; the last two categories overlapped almost perfectly. We generally saw little or no surface-localized fluorescence in treated cells. The number of cells showing nuclear uptake of carboxyfluorescein-labeled β-peptides was compared to the total number of cells as determined by transmission images. In each case, 70–100 cells were evaluated. Each data point shown in the figures represents an average of at least four separate experiments. Propidium iodide (PI) staining was used to detect dead or dying cells; PI-stained cells were not included in the cell counting data (i.e., there were no PI-stained cells among the 70–100 cells evaluated in a given experiment). In most cases we found that $<10\%$ of the cells treated with β-peptides were stained with PI, indicating that the β-peptides display little or no toxicity toward HeLa cells.

Expression of dynamin K44A in HeLa cells:[41,42] Subconfluent cells were plated onto 35 mm glass-bottomed culture dishes (MatTek; 10^5 cells per well) and cultured overnight in DMEM. A plasmid encoding dynamin-1 K44A was transfected into the cells with the aid of Lipofectamine 2000 (Invitrogen) or TranSit (Mirus). The cells were grown for 24 h and were then incubated with peptide (8 μM **1b**, **2b**, or **3b**) and TR-Tf (5 μg mL^{-1}) for 30 min at 37 °C. The cells were washed with PBS (3×2 mL) containing propidium iodide (4 μg), with a brief (5 min) incubation at 37 °C between wash steps. The cells were then viewed by confocal microscopy.

Amiloride treatment:[43–45] Cells plated to 10^5 per well in 35 mm MatTek dishes were incubated in DMEM with FBS (10%) and pen/strep for 24 h. The medium was removed and the cells were washed with PBS (2 mL) before being incubated with ethyl isopropyl amiloride (EIPA; 100 μM) in OptiMEM for 30 min at 37 °C. The medium was then replaced with carboxyfluorescein-labeled β-peptide (8 μM) and EIPA (100 μM) in OptiMEM, and the cells were incubated for 1 h at 37 °C. The cells were then washed with PBS (3× 2 mL) containing propidium iodide (4 μg), with a 5 min incubation at 4 °C between wash steps. The cells were then viewed by confocal microscopy. Mock-treated cells that had not been incubated with Opti-MEM containing EIPA were viewed in parallel.

Phalloidin staining:[3] Cells plated at a density of 5×10^4 per well in MatTek dishes were incubated in DMEM with FBS (10%) and pen/strep for 24 h. The medium was removed, and the cells were washed once with serum-free DMEM (2 mL). The cells were then serum starved for 24 h at 37 °C in serum-free DMEM. After 24 h, the cells were washed with serum-free DMEM, and the medium was replaced with unlabeled β-peptide (8 μM, **1a**, **2a**, or **3a**) or EGF (10 nM) in serum-free DMEM (500 μl) and incubated for 30 min at 37 °C. The cells were washed with PBS (3×2 mL), fixed in paraformaldehyde (4%) in PBS for 15 min at RT, washed with PBS (3× 2 mL) at RT, and permeabilized with Triton-X-100 (0.3% *w/v*) for 25 min at 4 °C. After washing with PBS (3×2 mL), the cells were incubated with BSA (1%) in PBS for 45 min at RT to prevent nonspecific binding of phalloidin to hydrophobic proteins in the cell. The cells were then stained with Alexa Fluor 488 phalloidin (1 μg mL^{-1}) in PBS for 45 min at RT. Excess phalloidin was removed with PBS (3×2 mL) and the cells were viewed by confocal microscopy.

Heparinase treatment:[46] Cells were plated and starved as described in the section on "Phalloidin staining" except that before treatment with β-peptide **1a** or EGF, cells were incubated for 40 min at 37 °C with heparinase III (10 milliunits) and were then washed with PBS (3×2 mL).

EGF stimulation of β-peptide uptake:[3] Cells were plated at a density of 10^5 per well and incubated for 24 h at 37 °C in DMEM with FBS (10%) and pen/strep. The cells were then washed with PBS (2 mL) before addition of OptiMEM (1 mL) containing either **2b** or **3b** (8 μM) or EGF (10 nM) and **2b** or **3b** (8 μM). After incubation for 1 h at 37 °C, the cells were washed with PBS (3×2 mL). The medium was then replaced with OptiMEM (2 mL), and the cells were incubated for 1 h at 37 °C. The cells were washed again with PBS (3×2 mL) and viewed by confocal microscopy. Uptake of **2b** and **3b** in the presence and absence of EGF was determined by cell counting.

Translocation of α and β-peptides into vesicles: Large unilamellar lipid vesicles (LUVs) were prepared as described previously[28] by dispersal of dried lipid mixtures in KCl (128 mM), MOPS-K^+ (10 mM), EDTA-K^+ (0.1 mM), pH 7.4 (K^+-buffer) or an equivalent buffer (Na^+-buffer) in which potassium ions were entirely replaced by sodium ions, and extrusion through polycarbonate filters (0.1 mm pore size). Potassium-loaded LUVs in Na^+-buffer were prepared by gel-filtering of vesicles, dispersed, and extruded in K^+-buffer, through columns of Sephadex G-75 equilibrated with Na^+-buffer. The fluorescence of NBD-labeled α and β-peptides was measured with a Perkin–Elmer LS-50B luminescence spectrometer with excitation and emission wavelengths of 470 nm and 538 nm, respectively (slit settings 10 nm in both channels).

The affinity of binding of NBD-labeled peptides to LUVs was determined by taking advantage of the fact that there is a large enhancement of NBD fluorescence when the fluorophore is associated with membranes. Replicate samples containing NBD-labeled peptide (0.1 nmol) and varying concentrations of lipid vesicles were first incubated for 30 min at 37 °C in Na^+-buffer (3 mL). The samples were then transferred to a stirred and temperature-regulated fluorimeter cuvette, and the initial fluorescence intensity (F_i) was determined. After 15 s, sonicated POPG vesicles (100 nmol lipid) were added, rapidly binding essentially 100% of the peptide molecules present in the sample, and the fluorescence was further monitored (typically for 1–3 min) until the signal intensity restabilized at some F_{PG} (fluorescence of POPG-bound peptide) value. The normalized fluorescence F_N was calculated as the ratio of the measured intensities (F_i/F_{PG}) and was plotted as a function of [Lipid]exp, the concentration of phospholipid to which the peptide has access (i.e., the concentration of phospholipid exposed at the vesicle outer surface) during the initial incubation of the peptide with the LUVs. The latter quantity was calculated from the concentration of added LUV phospholipid and the ratio of surface exposed to total

phospholipids, determined by the procedure of Nordlund et al.[44] as described previously.[28] The resulting curve was fitted to an equation of the form:

$$F_N = F_N^0 + (F_N^{max} - F_N^0) \cdot \frac{[lipid]_{exp}}{[lipid]_{exp} + K_d}$$

here K_d is the effective dissociation constant for peptide–vesicle binding and F_N^0 and F_N^{max} are the values of the normalized fluorescence for free and LUV-bound peptide, respectively.

Translocation of NBD-labeled peptide molecules into large unilamellar lipid vesicles was assayed by the dithionite-reduction method described previously,[28] with some modifications. Briefly, samples containing peptide (3 μM) and potassium-loaded vesicles (3 mM lipid) in Na^+ buffer were first preincubated for 15 min at 37 °C. An aliquot (30 μL) of the incubation mixture was removed and diluted into Na^+-buffer (3 mL) in a stirred fluorimeter cuvette, and the fluorescence was measured before (F_o) and after (F_{PG}) addition of sonicated POPG vesicles as described above to calculate the normalized fluorescence value F_N for the diluted oligomer/LUV sample. Valinomycin (1/200 000 mol/mol lipid) was then added to the remaining (concentrated) peptide/LUV incubation mixture, from which aliquots (30 μL) were withdrawn at various times and diluted into Na^+-buffer (3 mL) in the fluorimeter cuvette, and the fluorescence was determined before (F_o) and after (F_D) addition of freshly prepared sodium dithionite solution (1 M, 30 μL). From these fluorescence readings (after blank correction), the fluorescence value F_{max} expected if 100% of the peptide molecules were associated with the LUVs was first calculated, from the value of F_N^{max} determined (for the relevant lipid composition) from the binding experiments outlined in the previous paragraph. The extent of translocation of peptide molecules into LUV was then calculated from the value of F_D measured at each time point after addition of valinomycin, through the equation (% translocation) = (100%)·(F_D/F_{max}). Similar determinations were made of the extent of peptide translocation into vesicles lacking a transbilayer potential gradient, with vesicles prepared with Na^+ buffer inside and outside.

Abbreviations

ACHC: *trans*-2-aminocyclohexanecarboxylic acid, DMEM: Dulbecco's modified Eagle's medium, EGF: epidermal growth factor, EIPA: ethyl isopropyl amiloride, NBD: 7-nitrobenz-2-oxa-1,3-diazole-4-yl fluorophore, POPC: 1-palmitoyl-2-oleoyl: *sn*-glycero-3-phosphocholine, POPG: 1-palmitoyl-2-oleoyl: *sn*-glycero-3-phosphoglycerol, POPS: 1-palmitoyl-2-oleoyl: *sn*-glycero-3-phosphoserine, PI: phosphatidylinositol, TfR: transferrin receptor, DPC: dodecylphosphocholine.

Acknowledgements

This work was supported in part by NIH grants GM56414 (to S.H.G.) and GM55427 (to A.K.M.), and an operating grant (MOP-7776) from the Canadian Institutes of Health Research (to J.S.). We thank Alan Rapraeger for helpful discussions and Tim McGraw for comments on the manuscript.

Keywords: macropinocytosis · membranes · peptides · peptidomimetics · proteoglycans

[1] R. Fischer, M. Fotin-Mleczek, H. Hufnagel, R. Brock, *ChemBioChem* **2005**, *6*, 2126–2142.
[2] T. B. Potocky, A. K. Menon, S. H. Gellman, *J. Biol. Chem.* **2003**, *278*, 50188–50194.
[3] R. Fischer, K. Kohler, M. Fotin-Mleczek, R. Brock, *J. Biol. Chem.* **2004**, *279*, 12625–12635.
[4] I. Nakase, M. Niwa, T. Takeuchi, K. Sonomura, N. Kawabata, Y. Koike, M. Takehashi, U. K. Tanaka, J. C. Simpson, A. T. Jones, Y. Sugiura, S. Futaki, *Mol. Ther.* **2004**, *10*, 1011–1022.
[5] J. S. Wadia, R. V. Stan, S. F. Dowdy, *Nat. Med.* **2004**, *10*, 310–315.
[6] R. Trehin, U. Krauss, R. Muff, M. Meinecke, A. G. Beck-Sickinger, H. P. Merkle, *Pharm. Res.* **2004**, *21*, 33–42.
[7] C. Foerg, U. Ziegler, J. Fernandez-Carneado, E. Giralt, R. Rennert, A. G. Beck-Sickinger, H. P. Merkle, *Biochemistry* **2005**, *44*, 72–81.
[8] J. P. Richard, K. Melikov, H. Brooks, P. Prevot, B. Lebleu, L. V. Chernomordik, *J. Biol. Chem.* **2005**, *280*, 15300–15306.
[9] I. M. Kaplan, J. S. Wadia, S. F. Dowdy, *J. Controlled Release* **2005**, *102*, 247–253.
[10] T. B. Potocky, A. K. Menon, S. H. Gellman, *J. Am. Chem. Soc.* **2005**, *127*, 3686–3687.
[11] M. Nishihara, F. Perret, T. Takeuchi, S. Futaki, A. N. Lazar, A. W. Coleman, N. Sakai, S. Matile, *Org. Biomol. Chem.* **2005**, *3*, 1659–1669.
[12] P. S. Wender, J. B. Rothbard, T. C. Jessop, E. L. Kreider, B. L. Wylie, *J. Am. Chem. Soc.* **2002**, *124*, 13382–13383.
[13] S. Al-Taei, N. A. Penning, J. C. Simpson, S. Futaki, T. Takeuchi, I. Nakase, A. T. Jones, *Bioconjugate Chem.* **2006**, *17*, 90–100.
[14] M. Fretz, J. Jin, R. Conibere, N. A. Penning, S. Al-Taei, G. Storm, S. Futaki, T. Takeuchi, I. Nakase, A. T. Jones, *J. Controlled Release* **2006**, *116*, 247–254.
[15] S. Pujals, J. Fernández-Carneado, C. López-Iglesias, M. J. Kogan, E. Giralt, *Biochim. Biophys. Acta* **2006**, *1758*, 264–279.
[16] M. Magzoub, S. Sandgren, P. Lundberg, K. Oglecka, J. Lilja, A. Wittrup, L. E. G. Eriksson, U. Langlo, M. Belting, A. Gräslund, *Biochem. Biophys. Res. Commun.* **2006**, *348*, 379–385.
[17] J. L. Zaro, T. E. Rajapaksa, C. T. Okamoto, W. C. Shen, *Mol. Pharm.* **2006**, *3*, 181–186.
[18] T. Takeuchi, M. Kosuge, A. Tadokoro, Y. Sugiura, M. Nishi, M. Kawata, N. Sakai, S. Matile, S. Futaki, *ACS Chem. Biol.* **2006**, *1*, 299–303.
[19] M. Rueping, Y. Mahajan, M. Sauer, D. Seebach, *ChemBioChem* **2002**, *3*, 257–259.
[20] C. Garcia-Echeverria, S. Ruetz, *Bioorg. Med. Chem. Lett.* **2003**, *13*, 247–251.
[21] D. Seebach, K. Namoto, Y. R. Mahajan, P. Bindschädler, R. Sustmann, M. Kirsch, N. S. Ryder, M. Weiss, M. Sauer, C. Roth, S. Werner, H. D. Beer, C. Munding, P. Walde, M. Voser, *Chem. Biodiversity* **2004**, *1*, 65–97.
[22] P. S. Kabouridis, *Trends Biotechnol.* **2003**, *21*, 498–503.
[23] E. Vives, P. Brodin, B. Lebleu, *J. Biol. Chem.* **1997**, *272*, 16010–16017.
[24] J. L. Zaro, W. C. Shen, *Exp. Cell Res.* **2005**, *307*, 164–173.
[25] J. B. Rothbard, T. C. Jessop, R. S. Lewis, B. A. Murray, P. A. Wender, *J. Am. Chem. Soc.* **2004**, *126*, 9506–9507.
[26] B. Christiaens, J. Grooten, M. Reusens, A. Joliot, M. Goethals, J. Vandekerckhove, A. Prochiantz, M. Rosseneu, *Eur. J. Biochem.* **2004**, *271*, 1187–1197.
[27] P. E. Thorén, D. Persson, P. Isakson, M. Goksör, A. Önfelt, B. Nordén, *Biochem. Biophys. Res. Commun.* **2003**, *307*, 100–107.
[28] D. Terrone, S. L. Sang, L. Roudaia, J. R. Silvius, *Biochemistry* **2003**, *42*, 13787–13799.
[29] M. Magzoub, A. Pramanik, A. Gräslund, *Biochemistry* **2005**, *44*, 14890–14897.
[30] E. Bárány-Wallje, S. Keeler, S. Serowy, S. Beibel, P. Pohl, M. Bienert, M. Dathe, *Biophys. J.* **2005**, *89*, 2513–2521.
[31] R. P. Cheng, S. H. Gellman, W. F. DeGrado, *Chem. Rev.* **2001**, *101*, 3219–3232.
[32] T. L. Raguse, J. R. Lai, S. H. Gellman, *J. Am. Chem. Soc.* **2003**, *125*, 5592–5593.
[33] D. H. Appella, J. J. Barchi, S. R. Durell, S. H. Gellman, *J. Am. Chem. Soc.* **1999**, *121*, 2309–2310.
[34] D. Seebach, M. Overhand, F. N. M. Kuhnle, B. Martinoni, L. Oberer, U. Hommel, H. Widmer, *Helv. Chim. Acta* **1996**, *79*, 913–941.
[35] D. Seebach, J. L. Matthews, *Chem. Commun.* **1997**, *21*, 2015–2022.
[36] S. H. Gellman, *Acc. Chem. Res.* **1998**, *31*, 173–180.

[37] D. Seebach, A. K. Beck, D. J. Bierbaum, *Chem. Biodiversity* **2004**, *1*, 1111 – 1239.
[38] T. L. Raguse, E. A. Porter, B. Weisblum, S. H. Gellman, *J. Am. Chem. Soc.* **2002**, *124*, 12774 – 12785.
[39] Y. A. Fillon, J. P. Anderson, J. Chmielewski, *J. Am. Chem. Soc.* **2005**,*127*, 11798 – 11803.
[40] J. Farrera-Sinfreu, E. Giralt, S. Castel, F. Albericio, M. Royo, *J. Am. Chem. Soc.* **2005**, *127*, 9459 – 9468.
[41] H. Damke, T. Baba, D. E. Warnock, S. L. Schmid, *J. Cell Biol.* **1994**, *127*, 915 – 934.
[42] H. Damke, *FEBS Lett.* **1996**, *389*, 48 – 51.
[43] J. A. Swanson, C. Watts, C. *Trends Cell Biol.* **1995**, *5*, 424 – 428.
[44] B. A. Watts III, D. W. Good, *J. Biol. Chem.* **1994**, *269*, 20250 – 20255.
[45] O. Meier, K. Boucke, S. V. Hammer, S. Keller, R. P. Stidwill, S. Hemmi, U. F. Greber, *J. Cell. Biol.* **2002**, *158*, 1119 – 1131.
[46] M. Tyagi, M. Rusnati, M. Presta, M. Giacca, *J. Biol. Chem.* **2001**, *276*, 3254 – 3261.
[47] J. R. Nordlund, C. F. Schmidt, S. N. Dicken, T. E. Thompson, *Biochemistry* **1981**, *20*, 3237 – 3241.
[48] M. A. West, M. S. Bretscher, C. Watts, *J. Cell Biol.* **1989**, *109*, 2731 – 2739.
[49] J. M. Sanger, B. Mittal, J. S. Dome, J. W. Sanger, *Cell Motil. Cytoskeleton* **1989**, *14*, 201 – 219.
[50] S. Fuchs, R. T. Raines, *Biochemistry* **2004**, *43*, 2438 – 2444.
[51] J. A. Leifert, J. L. Whitton, *Mol. Ther.* **2003**, *8*, 13 – 20.
[52] M. Belting, *Trends Biochem. Sci.* **2003**, *28*, 145 – 151.
[53] S. Hakansson, M. Caffrey, *Biochemistry* **2003**, *42*, 8999 – 9006.
[54] A. Ziegler, X. L. Blatter, A. Seelig, J. Seelig, *Biochemistry* **2003**, *42*, 9185 – 9194.
[55] A. Ziegler, J. Seelig, *Biophys. J.* **2004**, *86*, 254 – 263.
[56] I. Nakase, A. Tadokoro, N. Kawabata, T. Takeuchi, H. Katoh, K. Hiramoto, M. Negishsi, M. Nomizu, Y. Sugiura, S. Futaki, *Biochemistry* **2007**, *46*, 492 – 501.

Received: December 22, 2006

